U.P.B. Sci. Bull., Series C, Vol. 84, Iss. 4, 2022 ISSN 2286-3540

DYNAMIC FLEXIBLE EXTENDED HARMONIC DOMAIN MODELING AND SIMULATION OF SWITCHED CIRCUITS

Uriel VARGAS[1], George-Cristian LAZAROIU[2]

Transient analysis and simulation of switched circuits require accurate models that permit to reproduce dynamics as close as possible to real components. This paper introduces the application of a novel technique named as dynamic flexible extended harmonic domain (DFEHD) by simulating a switched circuit, i.e., an RLC circuit supplied by harmonic and interharmonic sources. The DFEHD technique is seen as a block-function whose input consists on the state-space system and as output the simulation results. The main objective of this paper is to demonstrate the simplicity of simulating linear time-periodic systems via the block-function DFEHD. The proposed case study is validated via PSCAD/EMTDC.

Keywords: harmonics, interharmonics, linear time-periodic systems, transient simulation

1. Introduction

The increasing use of power electronic converters (PECs) is becoming a major issue due to the negative impact on power quality, i.e., PECs introduce distinct frequency spectrum superimposed into the fundamental frequency that may cause, e.g., harmonic distortion, flickering, incorrect tripping of circuit breakers, among others [1]-[5].

Linear time periodic (LTP) systems involving PECs can be modeled and simulated, in a straightforward manner, in time-domain (TD); however, as consequence of switching phenomenon, a very small time-step must be employed; thus, leading to a large simulation time [6]-[7]. If harmonics and interhamonics dynamics are of interest, the flexible extended harmonic domain (FEHD) represents a solid improvement as it provides a set of linear ordinary differential equations (ODEs) where state variables become vectors containing time-varying frequency coefficients [8]. This means that, besides obtaining instantaneous values, it provides also the corresponding frequency spectrum for those pre-selected FEHD frequencies [8].

[1] Prof., Dept. of Power Systems, University POLITEHNICA of Bucharest, Romania, e-mail: uriel.vargas@upb.ro
[2] Prof., Dept. of Power Systems, University POLITEHNICA of Bucharest, Romania, e-mail: cristian.lazaroiu@upb.ro

A major improvement, which represents the main focus of this paper, is the dynamic FEHD (DFEHD) [9]. DFEHD is able to achieve correct transient waveform of all frequency spectrum while using arbitrary time discretization for calculation of instantaneous waveforms. It is worth mentioning, on the other hand, that FEHD fails to provide accurate transient waveforms as only pre-selected harmonics and interharmonics are accounted for [8], not so for the DFEHD that actually represents the analytic solution of the LTP system [9].

A case study of a switched circuit, i.e., an *RLC* circuit supplied by harmonic and interharmonic sources, is presented. The calculated system model is introduced, in a straightforward manner, into the block-function DFEHD technique to obtain the simulation results. The waveforms obtained by the proposed approach are verified with the PSCAD/EMTDC software tool [10].

2. Dynamic flexible extended harmonic domain (DFEHD) basics

This section describes the fundamental relations of the DFEHD technique. On one side, FEHD resolves the set of ODEs by using a numerical integration method and provides as outcome the dynamics of a fixed set of pre-selected harmonic and/or interharmonic frequencies, and the corresponding instantaneous waveforms [8]. On the other hand, DFEHD transforms the analytic modal solution for linear systems with constant coefficients to the FEHD [9]. This combination permits to obtain the dynamics of a more complete set of frequencies, in addition to the pre-selected set of harmonics and/or interharmonics.

Another major feature of the analytic nature of DFEHD is that it permits to calculate any solution point along the time axis [9]. This allows to set a higher resolution for visualization purposes of instantaneous variables, for example, immediately after a step change occurs, and a lower resolution after transients disappear; thus, leading to substantial CPU savings.

2.1. DFEHD mathematical representation

Based on the linear systems theory, the analytical modal solution to a multiple-input multiple-output (MIMO) linear time-invariant (LTI) *g*-order system is given by:

$$x(t,t_o) = Pe^{J(t-t_o)}P^{-1}x_o + P\int_{t_o}^{t} e^{J(t-s)}P^{-1}u(s)ds. \quad (1)$$

In (1), P is the left eigenvector matrix, J represents the diagonal eigenvalue matrix, x_o corresponds to the initial conditions vector, and vector u contains the m inputs.

The eigenvalue matrix J is split into real α and imaginary β parts, as given by (2) (using Matlab notation).

$$J = diag(\alpha_1, \cdots, \alpha_g) + jdiag(\beta_1, \cdots, \beta_g). \tag{2}$$

Note that the set β represents the natural frequencies of the system in rad/s.

The analytic solution given by (1), which is applicable only to LTI systems, is extended to LTP systems via the FEHD transformation, which after some algebraic manipulations becomes the DFEHD relation, as given by (3).

$$\begin{aligned} X(t) &= \bar{P}\left\{diag\left[\left(\bar{P}^{-1}X_o\right)^T\right]\right\}e^{(\bar{\alpha}+j\bar{\beta})(t-t_o)} \\ &-\sum_m U_m \bar{P}\left\{diag\left[\left(\bar{P}^{-1}B_{o,m}\right)^T\right]\right\}W_m e^{(\bar{\alpha}+j\bar{\beta})t+\left(j\omega_m-\bar{\alpha}-j\bar{\beta}\right)t_o} \\ &+X_{FHD}, \end{aligned} \tag{3}$$

or, in compact form:

$$X(t,t_o) = M(t,t_o)e^{j\bar{\beta}t} + X_{FHD}, \tag{4}$$

where:

$$\begin{aligned} M(t,t_o) &= \bar{P}\left\{diag\left[\left(\bar{P}^{-1}X_o\right)^T\right]\right\}e^{\bar{\alpha}(t-t_o)}e^{-j\bar{\beta}t_o} \\ &-\sum_m U_m \bar{P}\left\{diag\left[\left(\bar{P}^{-1}B_{o,m}\right)^T\right]\right\}W_m e^{\bar{\alpha}(t-t_o)+\left(j\omega_m-j\bar{\beta}\right)t_o}. \end{aligned} \tag{5}$$

In (3) to (5) we have the following definitions: m corresponds to the number of input sources (exponentials and DC); ω_m is the angular frequency of the m^{th} input source in rad/s; vector X_{FHD} indicates the steady-state solution of the FEHD model, which includes only the FEHD pre-selected frequencies; the eigenvector matrix $\bar{P}$ is the FEHD counterparts of P; $B_{o,m}$ represents a DC-component column vector corresponding to the m^{th} input element within the input matrix B; and X_o is the initial conditions vector.

Also in (3) to (5),

$$W_m = \begin{bmatrix} \dfrac{1}{j\omega_m - \left(\bar{\alpha}_1 + j\bar{\beta}_1\right)} & 0 & 0 \\ 0 & \ddots & 0 \\ 0 & 0 & \dfrac{1}{j\omega_m - \left(\bar{\alpha}_{(2h_{\max}+1)g} + j\bar{\beta}_{(2h_{\max}+1)g}\right)} \end{bmatrix}. \tag{6}$$

The fact that (1) is transformed using the FEHD, as in (3), it permits to obtain the analytic solution of the set of pre-selected frequencies in the FEHD model. In addition, the solution vector in (3) provides the dynamics of the natural frequencies of the system. This results in improved transient waveforms either for an instantaneous variable or for a specific selected harmonic and/or interharmonic, as demonstrated in [9].

2.2. Time-domain instantaneous waveforms

As for visualization purposes, each of the g solution variables in (3) is converted to TD as in (7), where "•" stands for the scalar product and f indicates the FEHD pre-selected frequencies.

$$\begin{bmatrix} x_1(t) \\ \vdots \\ x_g(t) \end{bmatrix} = \left\{ \begin{matrix} \begin{bmatrix} X_{1,-h_{\max}} \\ X_{1,-h_{\max}+1} \\ \vdots \\ X_{1,h_{\max}-1} \\ X_{1,h_{\max}} \end{bmatrix} \bullet \begin{bmatrix} e^{j(2\pi f_{1,-h_{\max}})t} \\ e^{j(2\pi f_{1,-h_{\max}+1})t} \\ \vdots \\ e^{j(2\pi f_{1,h_{\max}-1})t} \\ e^{j(2\pi f_{1,h_{\max}})t} \end{bmatrix} \\ \vdots \\ \begin{bmatrix} X_{g,-h_{\max}} \\ X_{g,-h_{\max}+1} \\ \vdots \\ X_{g,h_{\max}-1} \\ X_{g,h_{\max}} \end{bmatrix} \bullet \begin{bmatrix} e^{j(2\pi f_{g,-h_{\max}})t} \\ e^{j(2\pi f_{g,-h_{\max}+1})t} \\ \vdots \\ e^{j(2\pi f_{g,h_{\max}-1})t} \\ e^{j(2\pi f_{g,h_{\max}})t} \end{bmatrix} \end{matrix} \right\}. \tag{7}$$

The closed-form relation for the instantaneous variable corresponding to the single-input single-output (SISO) linear system case is obtained by applying the corresponding scalar product in (7) to (4), giving:

$$\begin{aligned} x(t,t_o) = M(t,t_o) \bullet & \left[\begin{bmatrix} e^{j(2\pi f_{-h_{\max}})t} \\ e^{j(2\pi f_{-h_{\max}+1})t} \\ \vdots \\ e^{j(2\pi f_{h_{\max}})t} \end{bmatrix} \begin{bmatrix} e^{j\bar{\beta}_1 t} & e^{j\bar{\beta}_2 t} & \cdots & e^{j\bar{\beta}_{(2h_{\max}+1)g} t} \end{bmatrix} \right] \\ & + \begin{bmatrix} X_{-h_{\max}} \\ X_{-h_{\max}+1} \\ \vdots \\ X_{h_{\max}} \end{bmatrix}_{FHD} \bullet \begin{bmatrix} e^{j(2\pi f_{-h_{\max}})t} \\ e^{j(2\pi f_{-h_{\max}+1})t} \\ \vdots \\ e^{j(2\pi f_{h_{\max}})t} \end{bmatrix}. \end{aligned} \tag{8}$$

Relation (8) shows that the analytic solution for an instantaneous solution state variable of a linear system is expressed as a sum of exponentials (sinusoidal signals), whose frequencies are given in terms of the set of pre-selected FEHD frequencies, the set of natural frequencies from the analytical modal solution, and the combination of these two sets. This can be observed in a clearer way if (8) is rewritten as (9).

$$x(t,t_o) = \sum_{r=-h_{\max}}^{h_{\max}} \sum_{s=1}^{2h_{\max}+1} M_{r,s}(t,t_o) e^{j(2\pi f_r + \overline{\beta}_s)t} + \sum_{r=-h_{\max}}^{h_{\max}} X_{FHD}^{r} e^{j(2\pi f_r)t}. \quad (9)$$

3. Case Study: *RLC* circuit supplied by harmonic and interharmonic sources

This case study is modeled in the FEHD and simulated using the block-function DFEHD. The main objective is to demonstrate the simplicity of simulating FEHD models via the DFEHD. In this sense, the DFEHD technique is seen as a block-function whose input is the state-space FEHD system and as output the simulation results.

Aimed to verify and validate the proposed model, which is implemented in Matlab using a computer i5-6200U CPU, 2.3 GHz, and 8GB RAM, the obtained results are compared with those given by the PSCAD/EMTDC software tool [10].

3.1. General description

Consider the *RLC* circuit presented in Fig. 1, which is supplied by both harmonic and interharmonic sources. The corresponding system parameters are presented in Table 1.

Table 1

Data for *RLC* circuit supplied by harmonic and interharmonic sources.

R_1	0.25 Ω
R_3	0.05 Ω
L_1	3 mH
L_3	1 mH
C_2	220 μF
t_s	0.25 s
v_1 (V)	0.2 + 1.5 sin($\omega_1 t$ + 90°) + 0.3 sin($\omega_2 t$ + 120°) + 0.2 sin($\omega_3 t$ - 20°)
v_2 (V)	0.15 sin($\omega_4 t$ + 240°) + 0.05 sin($\omega_5 t$ - 80°)
i_1 (A)	- 0.3 + 0.25 sin($\omega_6 t$ + 30°)
ω_1	2π × (50 Hz)
ω_2	2π × (100 Hz)
ω_3	2π × (150 Hz)
ω_4	2π × (75 Hz)
ω_5	2π × (40 Hz)
ω_6	2π × (2000 Hz)

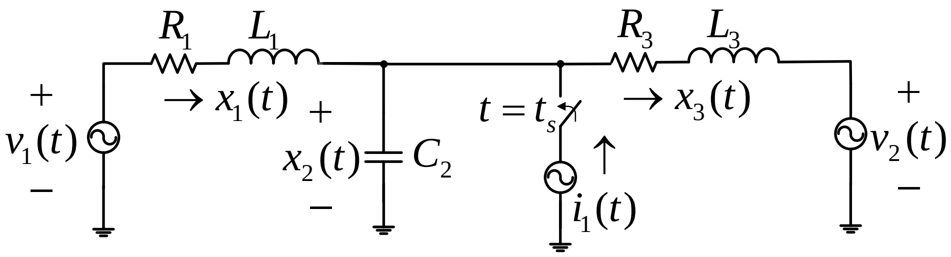

Fig. 1. *RLC* circuit supplied by harmonic and interharmonic sources.

Based on the reference directions in Fig. 1, the state-space representation of the *RLC* circuit is obtained in the FEHD as:

$$\dot{X}(t) + NX(t) = AX(t) + BU, \tag{10}$$

where N represents the differentiation matrix, arranged as a block-diagonal matrix, and u is a step unit function. Moreover, the time-periodic elements in matrices A, B, C and D become re-structured Toeplitz-type matrices given by the frequency content of outputs, inputs, and switching functions [8], as in (11) to (14).

$$A = \begin{bmatrix} -\frac{R_1}{L_1} & -\frac{1}{L_1} & 0 \\ \frac{1}{C_2} & 0 & -\frac{1}{C_2} \\ 0 & \frac{1}{L_3} & -\frac{R_3}{L_3} \end{bmatrix}, \tag{11}$$

$$B = \begin{bmatrix} \frac{1}{L_1} & 0 & 0 \\ 0 & \frac{1}{C_2} & 0 \\ 0 & 0 & -\frac{1}{L_3} \end{bmatrix}, \tag{12}$$

$$X(t) = \begin{bmatrix} X_1(t) \\ X_2(t) \\ X_3(t) \end{bmatrix}, \tag{13}$$

$$U = \begin{bmatrix} V_1 \\ I_i \ u(t - t_s) \\ V_2 \end{bmatrix}. \tag{14}$$

The solution vector X(t) in (10) and (13) represents an FEHD column vector involving the pre-selected harmonics and interharmonics in each state/part of the system. It is worth mentioning that, for this case study and for sake of illustration, the pre-selected frequencies for the FEHD model are the ones given by the sources, as listed in Table 1.

3.2. DFEHD as a block-function

For sake of illustration, Fig. 2 presents the schematic representation of the proposed approach that permits to simulate and provide the frequency spectrum of any LTP system modeled in the FEHD. The Matlab code representing the core of this approach, represented as the blue rectangle in Fig. 2, can be provided upon request to the authors.

In Fig. 2, the first two blocks on the left-hand-side, named as “TD” and “FEHD”, represent the TD and FEHD models of the LTP system under study, respectively. On the other hand, the third block, named “DFEHD”, represents the DFEHD block-function that provides as output, the analytic solution, frequency spectrum and instantaneous values of the LTP system under study.

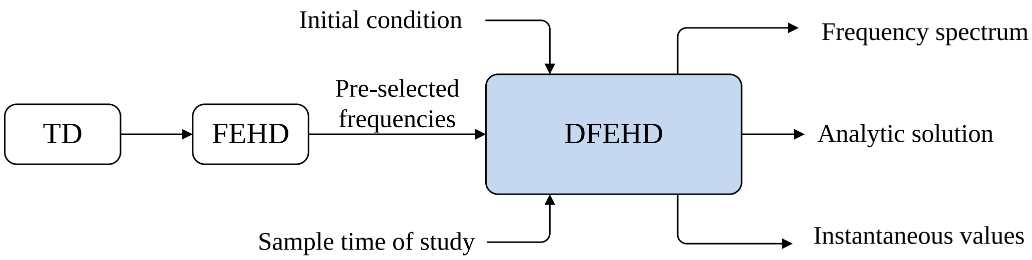

Fig. 2. DFEHD approach seen as a block-function.

3.3. Simulation results

Fig. 3 presents the instantaneous waveforms of x_1 and x_2, of Fig. 1, obtained by the proposed approach and by PSCAD/EMTDC.

To highlight the main feature of the DFEHD, which provides the analytic solution, i.e., it permits to calculate any solution point, four time-windows are used. The first time-window, $t \leq 0.05$ s, uses 500 linearly-spaced points; the second time-window, $0.05 \text{ s} \leq t \leq 0.25$ s, uses 50 linearly-spaced points; the third time-window, $0.25 \text{ s} \leq t \leq 0.35$ s, uses 1500 linearly-spaced points; and the fourth time-window, $0.35 \text{ s} \leq t \leq 0.5$ s, uses 50 linearly-spaced points. These solution points are shown in Fig. 3 via the “o” marker.

As observed in Fig. 3, the waveforms by the proposed DFEHD approach show an excellent agreement with PSCAD/EMTDC despite the arbitrary distribution of samples in the former. On the other hand, the higher switching frequency and/or source frequency, the smaller time-step required by PSCAD/EMTDC, which entails to a high computational burden.

For completeness of the paper, Fig. 4(a) presents the most representative frequencies of the highest distorted waveform, i.e., voltage at capacitor terminals x_2, whilst Fig. 4(b) shows its complete frequency spectrum in a 3D plot view.

From Fig. 4 we can observe all frequencies' participation given by the sources. In addition, we can easily visualize the natural frequency, which can be computed in Matlab using the TD or FEHD model and for this case study results in 391.7782 Hz. This natural frequency appears after every step change and decays exponentially as observed in Fig. 4. On the other hand, PSCAD/EMTDC models will be unable to show interharmonics accurately due to the dependency on the fast Fourier transform (FFT) algorithm, which in fact, is prone to incur in well-known errors, e. g., aliasing, spectral leakage, and Gibbs phenomenon [11]-[12].

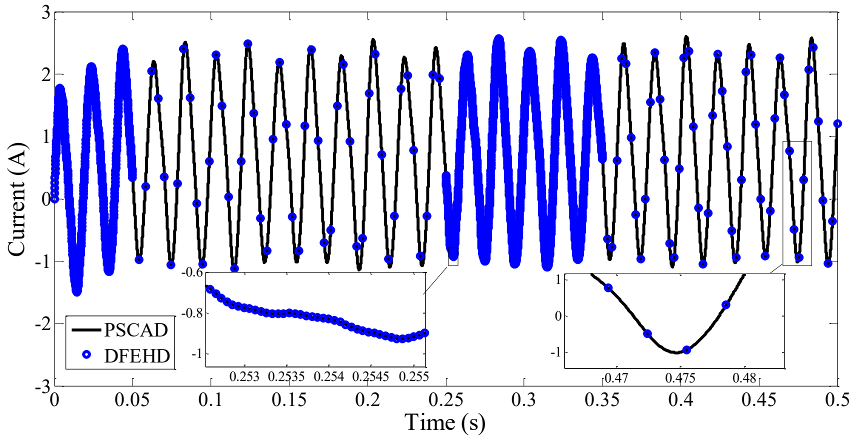

(a)

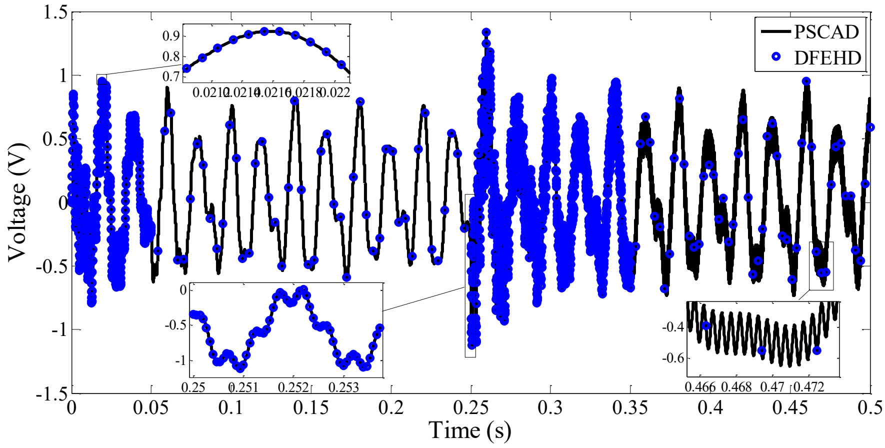

(b)

Fig. 3. Transient waveform for *RLC* case study. a) Current across inductor L_1. b) Voltage at capacitor terminals C_2.

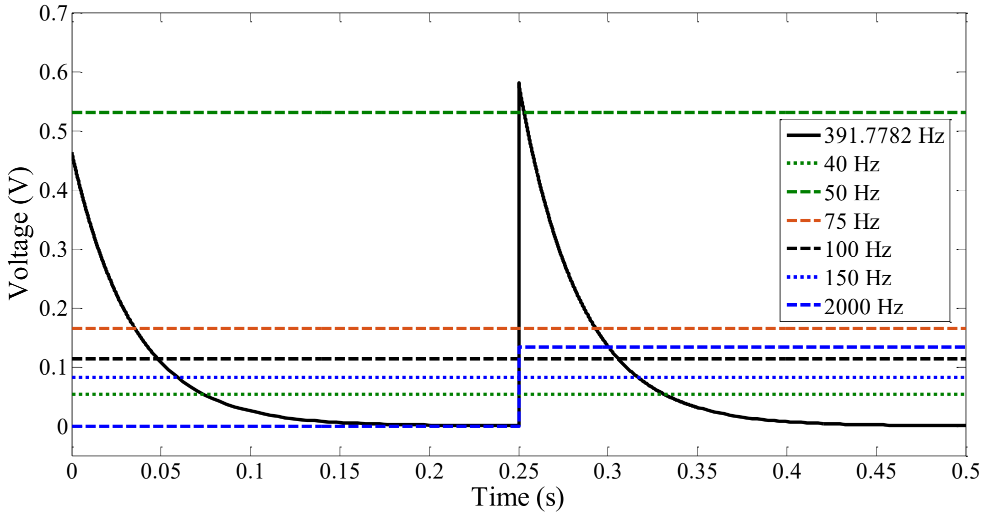

(a)

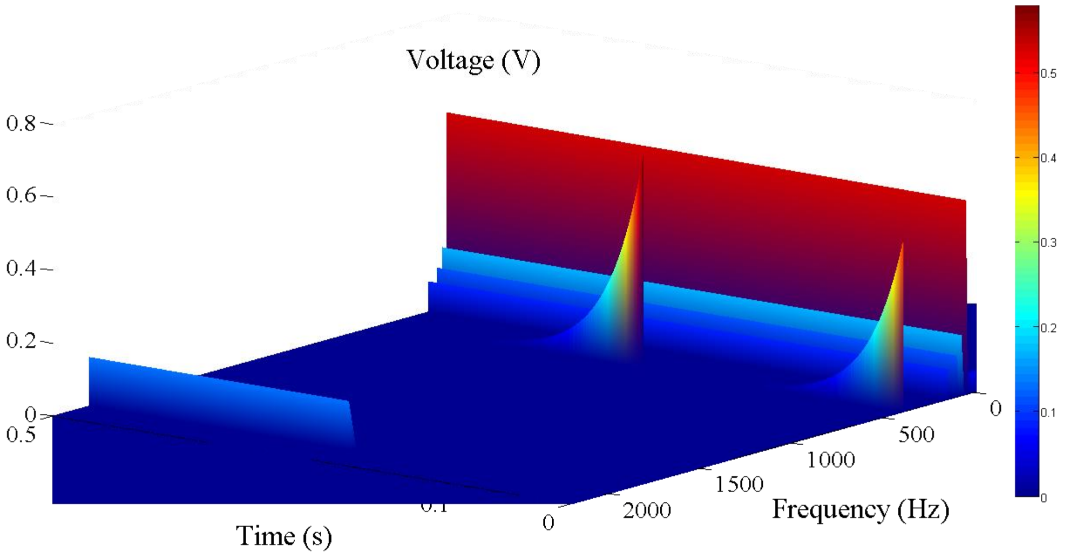

(b)

Fig. 4. Transient waveform for *RLC* case study. Frequency spectrum of voltage at capacitor terminals. a) 2D view. b) 3D view.

4. Conclusions

This paper has presented the DFEHD approach seen as a block-function, which provides, besides instantaneous values, the frequency evolution along time of any LTP system. This block-function has as inputs the FEHD model, initial condition, and the sample period under study whilst as outputs the analytic solution, instantaneous TD values and the frequency spectrum.

For simplicity of exposition, the proposed approach has been successfully validated via an *RLC* case study, where a remarkable accuracy can be observed; nevertheless, any LTP can be simulated, in a straightforward manner, using this methodology.

Four major features of the proposed approach can be mentioned: i) the analytic solution of any LTP system expressed as a sum of sinusoidal signals as output by the proposed block-function, ii) there is no need of numerical integration methods, iii) time-step independency as it permits to calculate any solution point along the time axis, and iv) it provides a complete frequency spectrum visualization.

Based on the aforementioned, the proposed methodology represents an alternative tool for evaluating or analyzing power quality in modern electrical LTP systems.

R E F E R E N C E S

[1]. *F. De la Rosa*, Harmonics and Power Systems, CRC press, USA, 2006.

[2]. *N. Golovanov. G. C. Lazaroiu, M. Roscia, D. Zaninelli*, Power quality assessment in small scale renewable energy sources supplying distribution systems, Energies, **vol. 6**, 2013, pp. 634-645.

[3]. *A. Testa, M.F. Akram, R. Burch, G. Carpinelli, G. Chang, V. Dinavahi, C. Hatziadoniu, W.M. Grady, E. Gunther, M. Halpin, P. Lehn, Y. Liu, R. Langella, M. Lowenstein, A. Medina, T. Ortmeyer, S. Ranade, P. Ribeiro, N. Watson, J. Wikston, W. Xu*, Interharmonics: Theory and modeling, **vol. 22**, 2007, pp. 2335-2348.

[4]. *M. Bollen, F. Hassan*, Integration of distributed generation in the power system, John Wiley & Sons, USA, 2011.

[5]. *E. Acha, M. Madrigal*, Power Systems Harmonics, Wiley, USA, 2001.

[6]. *S. R. Sanders, J. M. Noworolski, X. Z. Liu, G. C. Verghese*, Generalized Averaging Method for Power Conversion Circuits, IEEE Trans. Power Electron., **vol. 6**, 1991, pp. 251-259.

[7]. *U. Vargas, G. C. Lazaroiu, E. Tironi, A. Ramirez*, Harmonic modeling and simulation of a stand-alone photovoltaic-battery-supercapacitor hybrid system, Int. J. Electr. Power Energy Syst., **vol. 105**, 2019, pp. 70-78.

[8]. *U. Vargas, A. Ramirez, G. C. Lazaroiu*, Flexible extended harmonic domain approach for transient state analysis of switched systems, Electr. Power Syst. Res., **vol. 155**, 2018, pp. 40-47.

[9]. *U. Vargas, G. C. Lazaroiu, A. Ramirez,* Closed-Form calculation of linear Time-Periodic systems via the dynamic flexible extended harmonic domain, Int. J. Electr. Power Energy Syst., **vol. 143**, 2022.

[10]. Manitoba HVDC Research Centre Inc. Winnipeg, MB, Canada, free version.

[11]. *J. Proakis, D. Manolakis*, Digital SIgnal Processing, 2014.

[12]. *G. T. Heydt, P. S. Fjeld, C. C. Liu, D. Pierce, L. Tu, G. Hensley*, Applications of the windowed FFT to electric power quality assessment, IEEE Trans. Power Deliv., **vol. 14**, 1999, pp. 1411-1416.